

Direct Observation of the Charge-Density Wave in Potassium by Neutron Diffraction

T. M. Giebultowicz,^{(1),(2)} A. W. Overhauser,⁽²⁾ and S. A. Werner^{(1),(3)}

⁽¹⁾National Bureau of Standards, Gaithersburg, Maryland 20899

⁽²⁾Department of Physics, Purdue University, West Lafayette, Indiana 47907

⁽³⁾Department of Physics and Astronomy, University of Missouri, Columbia, Missouri 65211

(Received 13 January 1986)

Sharp charge-density-wave satellites in potassium have been located at (0.995, 0.975, 0.015). They are smaller than the {110} reflections by $\sim 10^5$, and each is surrounded by a prolate ellipsoidal cloud of diffuse phason scattering having its major axis along a line through the point (1,1,0).

PACS numbers: 61.55.Fe, 61.12.Gz, 71.45.Gm, 72.15.Nj

We announce discovery of the charge-density-wave (CDW) satellites in potassium. CDW instability of conduction electrons in a simple metal is a many-body effect, driven by exchange¹ and correlation.² Nevertheless, neutrons can interact with this charge modulation because a parasitic, periodic lattice distortion $A\hat{\epsilon}\sin\mathbf{Q}\cdot\mathbf{r}$ arises to provide charge neutralization.² Theoretical prediction and experimental evidence requires A to be so small,³ ~ 0.03 Å, and \mathbf{Q} to be so near the reciprocal lattice vector \mathbf{G}_{110} ,⁴ that finding the diffraction satellites at $\mathbf{G}_{hkl} \pm \mathbf{Q}$ is extremely difficult. Diffraction searches require a triple-axis spectrometer so that neutron energy transfer can be set equal to zero, providing thereby the needed isolation from inelastic phonon scattering.

The satellite structure we present here was obtained at 4.2 K, near [110], and with 4.08- and 4.70-Å neutrons. The beam was filtered with 6 in. of Be at 78 K. [An additional 6 in. of Be did not change the satellite-to-(110) intensity ratio, which confirmed that order contamination was unimportant.] We have studied the satellites for several years on four triple-axis spectrometers (at the National Bureau of Standards' research reactor), with five wavelengths from 2.35 to 4.70 Å, and near the [110], [220], [200], and [211] Bragg reflections. Highest resolution is obtained near [110] because the pyrolytic-graphite {002} monochromator spacing nearly matches that of potassium {110}.

Although each microscopic region of a potassium crystal has a single \mathbf{Q} ,⁵ there are 24 \mathbf{Q} domains in bulk and, consequently, 48 satellites near every hkl reflection.⁶ Most of these are swamped by background (near the Ewald sphere of reflection) caused by mosaic distribution. Others have small intensity because the lattice-displacement vector $\hat{\epsilon}$ is nearly perpendicular to the neutron scattering vector. We define the major satellites to be the family (one of six) for which Q_i , $i = 1, 2, 3, 4$, is nearly parallel to [110]. A satellite map in the $(\bar{1}\bar{1}0)$ plane near [110] is shown in Fig. 1. Each satellite is surrounded by a diffuse cloud of phason scattering, which redistributes the anticipated intensity.⁴ A previous search⁷ for CDW's in potassium did not probe this region, so close to the (110) point.

The single crystal used was a cylinder 2 cm in diameter and 7 cm long. It was sealed in a He-filled Al can and supported only by compressed quartz wool at each end. It was an exquisite specimen, having a mosaic

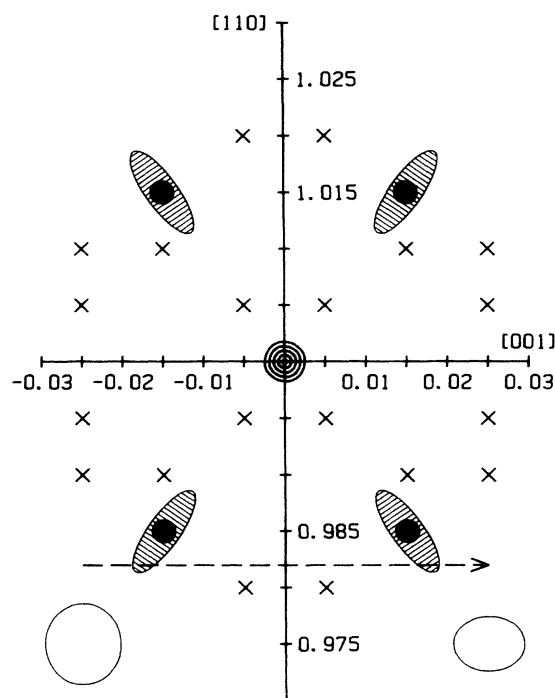


FIG. 1. Map of the $(\bar{1}\bar{1}0)$ scattering plane surrounding the [110] Bragg peak. The black dots are the main CDW satellites: The lower two come from the origin, [000], and the upper two from the [220]. The twenty crosses mark satellite locations generated by other nearby reciprocal-lattice vectors. Each point in the figure is the projection of two satellites (located slightly above and below the plane). The shaded ellipses represent diffuse phason scattering. The dashed line represents a transverse hhq scan having $h = 0.982$. The open ellipse in the lower left-hand corner is the experimental resolution for $\lambda = 4.08$ Å, collimation 40'-20'-20'-40', and energy resolution 0.15 meV. The other ellipse was measured with $\lambda = 4.70$ Å, collimation 20'-20'-20'-20', and energy resolution 0.07 meV, and pertains to the data in Fig. 5.

width of less than 0.1° in three mutually perpendicular planes. All rocking curves were free of structure. It was grown from potassium having a residual resistance ratio of ~ 8000 . (The bcc lattice constant of potassium at 4 K is $a = 5.2295 \text{ \AA}$.⁸)

Transverse hhq scans in the $(1\bar{1}0)$ plane which reveal CDW structure are presented in Fig. 2. The shaded inset is a similar scan through $[110]$; it shows that the CDW satellites are extremely sharp, almost equal in sharpness to the Bragg reflections. Inelastic phason scattering suffices to explain any excess width. Observe that for $h = 0.975$ the satellite peaks occur at $q = \pm 0.022$. As h increases this separation decreases and, within experimental error, the maxima lie along lines through $[110]$. For shorter neutron wavelength (and poorer h resolution), this tilt of the phason ellipsoid is less apparent. (Convolution of the resolution function with the final CDW structure distribution explains such behavior.) Three more transverse hhq scans, with trajectories closer to the $[110]$, are shown in Fig. 3. The peak heights of the CDW diffraction continue to increase, but the effect of the nearby $[110]$ grows very rapidly, causing the peak centered at $q = 0$.

Each satellite peak in Figs. 2 and 3 arises from a pair, one above and the other below the $(1\bar{1}0)$ scatter-

ing plane. The sample was reoriented in order to measure the satellite separations along the $[1\bar{1}0]$ direction. The sample was first rotated by 90° about the original $[110]$ scattering direction. The $[001]$ direction was then perpendicular to the (new) scattering plane. For reasons of beam geometry the sample was then rotated 90° about the (new) vertical direction. A series of twelve scans were made in this (001) plane. Three of these and the final map for the (001) plane are shown in Fig. 4. The major satellites depicted here correspond to Q domains for points $h = 0.990, q = \pm 0.015$, and $h = 1.010, q = \pm 0.015$ in Fig. 1. Once again the major axes of phason scattering appear to pass through $[110]$. The intensity reversal between scans *A* and *B* of Fig. 4 is not surprising. The peaks on the right- and left-hand sides of a given scan need not be equal, since they arise from different Q domains. However the Q domains which cause the right-hand peak in scan *A* cause the left-hand peak in scan *B*. A similar (but less dramatic) asymmetry reversal can be noticed in the upper two scans of Fig. 2.

Close approach to the $[110]$ requires longer wavelength and tighter collimation. Three higher-resolution scans are shown in Fig. 5. The price paid was a sixteenfold reduction in counting rate. However, com-

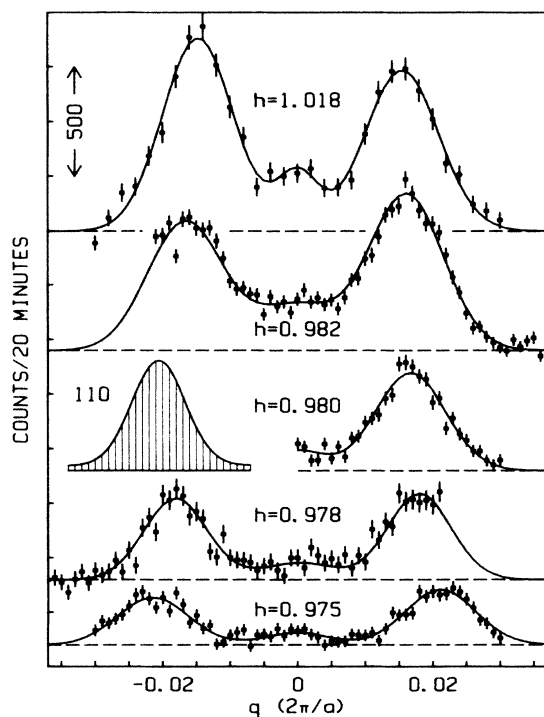


FIG. 2. Transverse hhq scans through the CDW structure in the $(1\bar{1}0)$ plane. The shaded inset is a scan through the $[110]$ peak, after normalizing the data by 1.5×10^{-5} . (Potassium, 4.2 K, $\lambda = 4.08 \text{ \AA}$.) The curves through the data are three-Gaussian optimum fits. Background lines have been positioned for clarity.

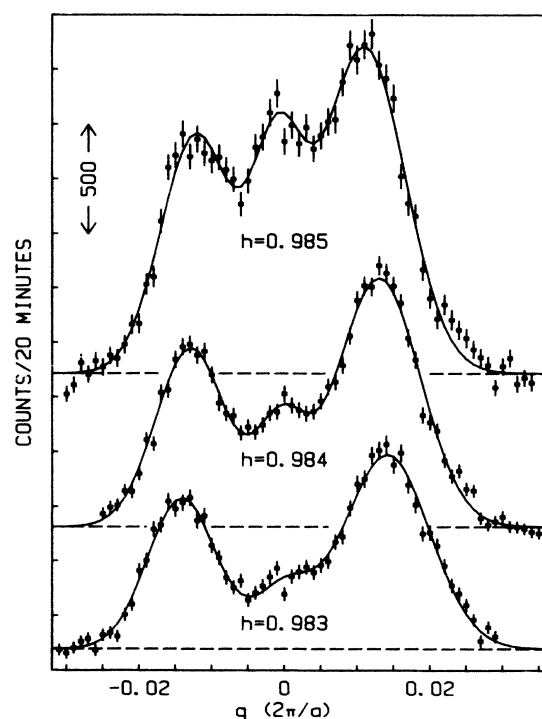


FIG. 3. Transverse scans in the $(1\bar{1}0)$ plane near the maxima of the CDW structure. The rapidly increasing component (vs h) at $q = 0$ is caused by the intense $[110]$. (Potassium, 4.2 K, $\lambda = 4.08 \text{ \AA}$.) The curves through the data are three-Gaussian optimum fits. Background lines have been positioned for clarity.

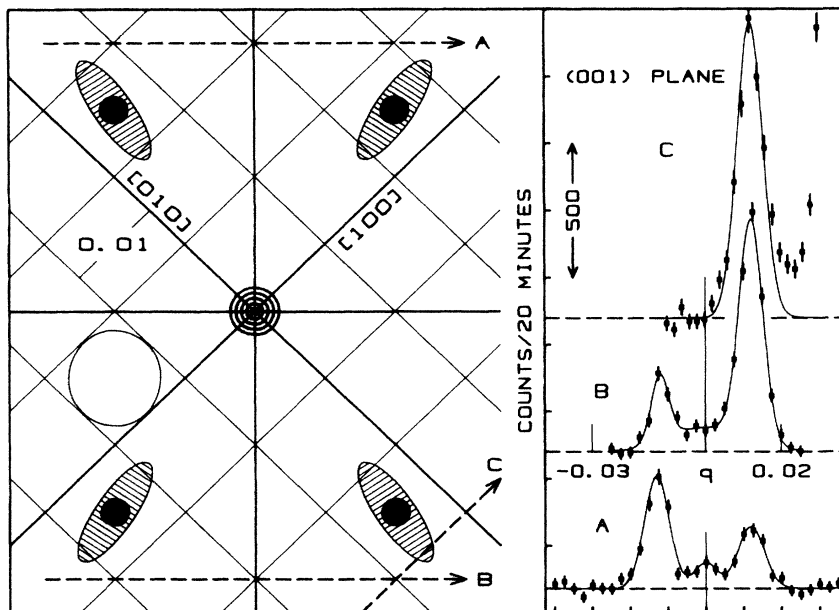


FIG. 4. Map of the (001) scattering plane near the [110] Bragg peak. On the right are three scans through the CDW structure indicated by the dashed lines on the left. *A* is $(1.02 + q, 1.02 - q, 0)$. *B* is $(0.98 + q, 0.98 - q, 0)$. *C* is $(0.936 + q, 0.97, 0)$. The rapidly rising background at the end of scan *C* is mosaic "splash," which occurs on approaching the Ewald sphere of reflection (at $1.03, 0.97, 0$), where the 20-minute count reached 4×10^4 . (The Bragg-peak count was 3×10^7 .) Curves for *A* and *B* are three-Gaussian optimum fits. (Potassium, 4.2 K, $\lambda = 4.08 \text{ \AA}$.)

parison of the $h = 0.985$ scans of Figs. 3 and 5 shows that the needed resolution was achieved. These high-resolution scans allow determination of the CDW satellite coordinate along the [110] scattering direction. A plot of the integrated intensities of all transverse hq scans versus h is also shown in Fig. 5. (Intensities from the peaks

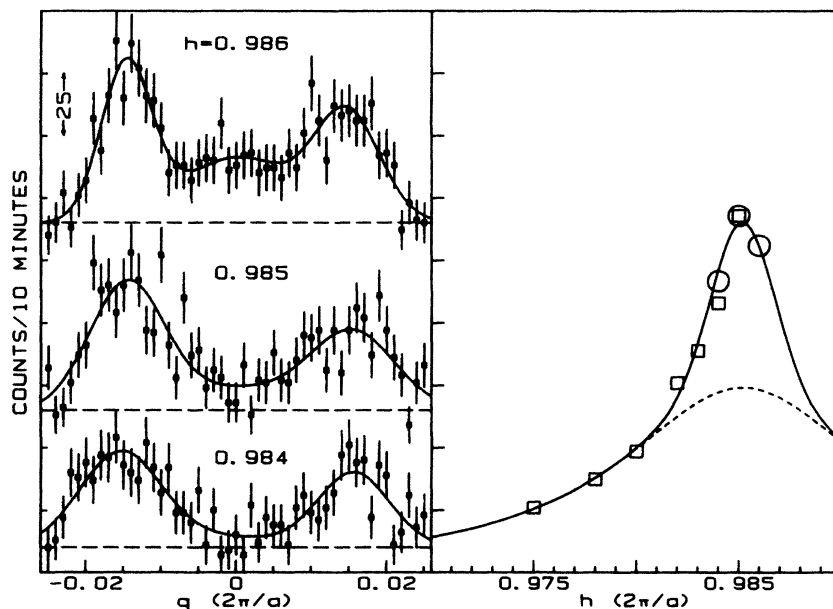


FIG. 5. High-resolution transverse hq scans near the maxima of the CDW satellites. $\lambda = 4.70 \text{ \AA}$. The seven squares in the right-hand panel are the integrated intensities of the CDW components from Figs. 2 and 3. The three circles are integrated intensities of the CDW components from the data on the left-hand side. A scale factor of 16 was used to force coincidence of the two points at $h = 0.985$. The solid curves in the left-hand panel are three-Gaussian optimum fits. The solid curve in the right-hand panel is the sum of a Gaussian and a Lorentzian. The sizes of the circles and squares represent our estimate of the relative precision.

at $q=0$ were subtracted.) The coordinate of the "maximum" scan is $h=0.985$. The curve through the integrated-intensity data was taken to be the sum of a Gaussian and a Lorentzian. Such a decomposition is purely heuristic. At present this is our best attempt to estimate the ratio of total intensities from elastic and phason contributions. The ratio found was about 1:7.

A series of constant-energy hhq scans were made at $h=0.970$. These CDW peaks were essentially all of phason origin. Neutron energy transfer was varied between $\Delta E = -0.5$ and 0.5 meV. The (phason) satellites reached their maxima at $\Delta E = 0.3$ meV, i.e., ~ 3.5 K. This value confirms the phason characteristic temperature (the phason analog of θ_D) found from analyses of resistivity,⁹ point-contact spectroscopy,¹⁰ and heat-capacity¹¹ data. A crucial experiment for the future would be a measurement of how much of the phason scattering is "pulled back" into the elastic peak at $T \sim 0.3$ K.

The structure we report cannot arise from phonons or Huang scattering, i.e., from frozen phonons caused by lattice imperfections. We have convolved the (four-dimensional) experimental resolution with the (known) lattice dynamics of potassium. The calculation was normalized to the measured intensity of the longitudinal phonon at (1.1,1.1,0). The resulting scattering function was too small by an order of magnitude, and had no sharp features resembling our data. Phonon scattering having energies less than 0.07 meV would increase by almost a factor of 20 at 78 K. This temperature independence is expected for CDW satellites since the resolution ellipsoid of the spectrometer (for this particular experiment) was larger than the phason ellipsoids shown in Fig. 1. The anisotropy of Huang scattering is similar to that from phonons, and cannot explain the sharp satellites we observe.

The CDW wave vector \mathbf{Q} determined by the data, with a precision of ~ 0.0004 for each component, is

$$\mathbf{Q} = (0.995, 0.975, 0.015). \quad (1)$$

The magnitude is $Q = 1.393(2\pi/a)$, which compares well with¹²

$$Q \approx 2k_F(1 + g/4E_F), \quad (2)$$

where g is the CDW energy gap (0.62 eV) and E_F is the experimental Fermi energy (1.5 eV).¹³ Equation (2) leads to $Q \approx 1.37(2\pi/a)$. The angle between \mathbf{Q}

and [110] is 0.85° . The theory⁶ of this tilt predicts 1.0° if the experimental $|\mathbf{Q}|$ is employed. The expected intensity of a satellite is 1.4×10^{-5} of the Bragg reflection.³ A tight quantitative comparison cannot be made because the [110] reflection is reduced by extinction. The CDW satellites are also reduced by phason scattering.⁴ Since these two corrections tend to compensate, the observed intensity ratio has approximately the predicted value.

Conduction electrons in potassium exhibit many anomalous properties attributable to static and dynamic effects of a CDW.^{14,15} Our diffraction data show that neutrons traversing metallic potassium provide direct evidence of the underlying phenomenon.

We are grateful to a number of colleagues, particularly to J. A. Gotaas, J. J. Rhyne, and J. M. Rowe, for assistance and counsel during the course of this investigation. We also thank the National Science Foundation for major support provided through the Materials Research Laboratory Program.

¹A. W. Overhauser, Phys. Rev. **128**, 1437 (1962).

²A. W. Overhauser, Phys. Rev. **167**, 691 (1968).

³G. F. Giuliani and A. W. Overhauser, Phys. Rev. B **22**, 3639 (1980).

⁴A. W. Overhauser, Phys. Rev. B **3**, 3172 (1971).

⁵A. W. Overhauser and N. R. Butler, Phys. Rev. B **14**, 3371 (1976).

⁶G. F. Giuliani and A. W. Overhauser, Phys. Rev. B **20**, 1328 (1979).

⁷S. A. Werner, J. Eckert, and G. Shirane, Phys. Rev. B **21**, 581 (1980).

⁸S. A. Werner, E. Gürmen, and A. Arrott, Phys. Rev. **186**, 705 (1969).

⁹Marilyn F. Bishop and A. W. Overhauser, Phys. Rev. B **23**, 3638 (1981).

¹⁰M. Ashraf and J. C. Swihart, Phys. Rev. Lett. **50**, 921 (1983).

¹¹C. D. Amarasekara and P. H. Keesom, Phys. Rev. B **26**, 2720 (1982).

¹²A. W. Overhauser, Phys. Rev. Lett. **13**, 190 (1964).

¹³E. Jensen and E. W. Plummer, Phys. Rev. Lett. **55**, 1912 (1985), and personal communication.

¹⁴A. W. Overhauser, Adv. Phys. **27**, 343 (1978).

¹⁵A. W. Overhauser, in *Highlights in Condensed Matter Theory*, International School of Physics "Enrico Fermi," Course 89, edited by F. Bassani, F. Fumi, and M. P. Tosi (North-Holland, Amsterdam, 1985), p. 194.